The Mechanism of Binding Staphylococcal Protein A to Immunoglobin G Does Not Involve Helix Unwinding†

Lena Jendeberg,‡,§ Mitsuru Tashiro,|| Roberto Tejero,||,⊥ Barbara A. Lyons,|| Mathias Uhlén,‡ Gaetano T. Montelione,*,|| and Björn Nilsson*,§

Department of Biochemistry and Biotechnology, Royal Institute of Technology, S-100 44 Stockholm, Sweden, Department of Structural Biochemistry, Pharmacia & Upjohn AB, S-112 87 Stockholm, Sweden, Center for Advanced Biotechnology and Medicine and Department of Molecular Biology and Biochemistry, Rutgers University, Piscataway, New Jersey 08854-5638, and Departamento de Quimica Fisica, Fac. Quim., Universidad de Valencia, Dr. Moliner 50. 46100 Burjassot, Valencia, Spain

Received June 8, 1995; Revised Manuscript Received September 11, 1995⊗

ABSTRACT: Structural changes in staphylococcal protein A (SpA) upon its binding to the constant region (Fc) of immunoglobulin G (IgG) have been studied by nuclear magnetic resonance and circular dichroism (CD) spectroscopy. The NMR solution structure of the engineered IgG-binding domain of SpA, the Z domain (an analogue of the B domain of SpA), has been determined by simulated annealing with molecular dynamics, using 599 distance and dihedral angle constraints. Domain Z contains three α-helices in the polypeptide segments Lys[7] to His[18] (helix 1), Glu[25] to Asp[36] (helix 2), and Ser[41] to Ala[54] (helix 3). The overall chain fold is an antiparallel three-helical bundle. This is in contrast to the previously determined X-ray structure of the similar SpA domain B in complex with Fc, where helix 3 is not observed in the electron density map [Deisenhofer, J. (1981) *Biochemistry 20,* 2361−2370], but simlar to the solution NMR structure of domain B, which is also a three-helical bundle structure [Gouda, H., et al. (1992) *Biochemistry 31,* 9665−9672]. In order to characterize possible secondary structural changes associated with IgG binding, far-UV CD spectra were collected for the Z domain, an engineered repeat of this molecule (ZZ), recombinant Fc from IgG subclass 1 (Fc_1), recombinant Fc from IgG subclass 3 (Fc_3), and mixtures of Z/Fc_1, Z/Fc_3, ZZ/Fc_1, and ZZ/Fc_3. Fc_3 was included as a control for possible changes of the CD spectrum in the mixture of noncomplexed molecules, since SpA is known not to bind Fc_3. From these CD spectra, it was concluded that the third α-helix in Z is *not* disrupted in its complexes with Fc_1. Similar results were obtained for the ZZ molecule. However, in both Z and ZZ there are some perturbations in CD spectra at high energy wavelengths (i.e., $\lambda < 215$ nm) accompanying complex formation. On the basis of the combined CD and NMR results, as well as previously described binding studies of Z mutant proteins to Fc_1, we conclude that the Z domain maintains its three-helical bundle structure in the Z−Fc complex, though there may be a small structural change involved in the binding mechanism.

SpA[1] is a cell-wall-bound pathogenicity factor from the bacterium *Staphylococcus aureus*. Its amino acid sequence consists of five homologous IgG-binding domains (from the N-terminus; E, D, A, B, and C), followed by the C-terminal cell-wall-binding region X (Deisenhofer, 1981; Langone, 1982; Uhlén et al., 1984). We, and others, are studying details in the interaction between staphylococcal protein A (SpA) and the constant (Fc) portion of human immunoglobulin class G (IgG) (Nilsson et al., 1987; Jansson et al., 1989; Torigoe et al., 1990a,b; Gouda et al., 1992; Cedergren et al., 1993; Ljungberg et al., 1993). The purpose of these studies is to dissect the importance of individual amino acid residues and the possible role of conformational rearrangements in the molecular recognition energy and mechanism. SpA−IgG interactions are potential targets for rational drug design and provide a model system for understanding atomic details of interactions between α-helical proteins and their IgG-like receptors common to a large number of analogous cytokines and growth factors (Bazan, 1990; Cunningham & Wells, 1993; Rozwarski et al., 1994).

The X-ray cocrystal structure of domain B in complex with the constant domain (Fc_1) of IgG subclass 1 has been solved at a resolution of 2.8 Å (Deisenhofer et al., 1976, 1978, 1981). The structure of domain B in the complex shows two antiparallel α-helices in contact with IgG. Nine amino acid residues in the Fc domain and 11 residues in domain B contribute to the binding surface between the two molecules. Unfortunately, the electron density for the C-terminal portion of domain B (i.e., residues 40−58) was very weak and difficult to interpret in the cocrystal structure (Deisenhofer et al., 1978, 1981).

Recently, a medium resolution structure of domain B in solution has been determined by NMR spectroscopy (Gouda et al., 1992). This structure reveals an antiparallel three-helix bundle motif. Thus, the C-terminal residues of

†This project has been financially supported by the National Institutes of Health (GM-47014), the National Science Foundation (Young Investigator Award MCB-9357526 to G.T.M. and MCB-9407569), Nutek, and Pharmacia & Upjohn AB.

* Corresponding authors.
‡ Royal Institute of Technology.
§ Pharmacia & Upjohn AB.
|| Rutgers University.
⊥ Universidad de Valencia.

⊗ Abstract published in *Advance ACS Abstracts,* December 1, 1995.

[1] Abbreviations: Fc_1, Fc fragment of immunoglobulin G subclass 1; Fc_3, Fc fragment of immunoglobulin G subclass 3; NOESY, nuclear Overhauser effect spectroscopy; PFG-HSQC, pulse-field gradient 2D heteronuclear correlation spectroscopy; SpA, staphylococcal protein A; Z, an IgG-binding domain derived from domain B of staphylococcal protein A; ZZ, a tandem repeat dimer of Z.

0006-2960/96/0435-22$12.00/0

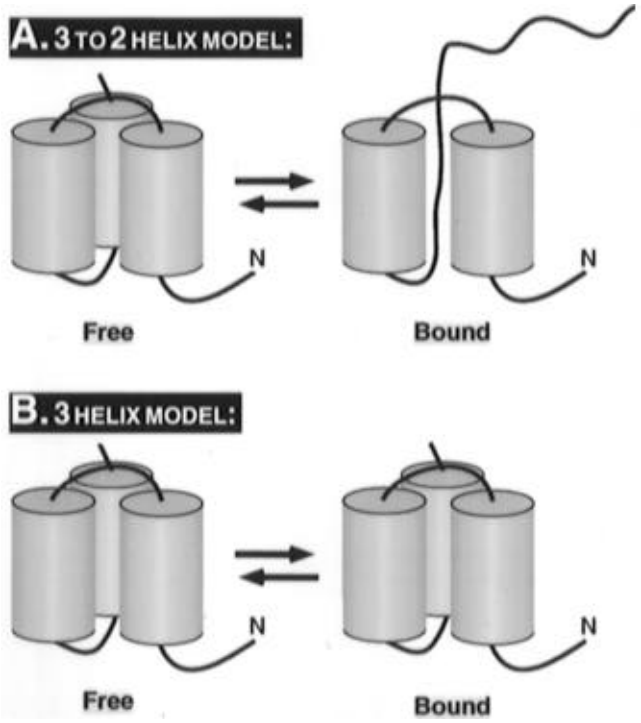

FIGURE 1: (A) Hypothetical binding mechanism involving "helical unwinding" of an IgG-binding SpA domain in the interaction with the Fc portion of immunoglobulins (Torigoe et al., 1990a). In solution (Free), the SpA domain is a three-helix bundle structure. In this model, the third α-helix is disrupted in the complexed SpA domain (Bound). (B) Alternative hypothetical binding mechanism preserving the overall three-helical bundle chain fold in the interaction of an IgG-binding SpA domain with the Fc portion of immunoglobulins. This alternative hypothesis includes the possibility of minor structural changes in relative orientations of the three helices in going from the free to bound states.

polypeptide segment Ser^{41}−Ala^{54} in domain B, which were not observed in the X-ray structure, were identified as an α-helix in the solution NMR structure. The discovery of this third helix in the solution structure resulted in a proposal that the third helix is disrupted upon binding to Fc (Torigoe et al., 1990a). This hypothesis, summarized in Figure 1, was further supported by a demonstrated difference in the nitrogen-15 chemical shift of residue Pro^{38}, situated in the loop region between helix 2 and helix 3, upon binding to Fc (Torigoe et al., 1990b). However, in a subsequent hydrogen-exchange study, it was found that several backbone amide protons within the polypeptide segment Leu^{45}−Ala^{54}, corresponding to the third helix, are protected from rapid hydrogen/deuterium exchange both in the free domain B and in the B−Fc$_1$ complex (Gouda et al., 1992), indicating that the third helix is in fact intact in this complex (Figure 1B). While consistent with intramolecular hydrogen bonds of an intact third helix of domain B in the B−Fc$_1$ complex, it is also possible that this amide-exchange protection results from intermolecular hydrogen bonds between the B domain and the Fc$_1$ molecule itself. Accordingly, the existing spectroscopic data (Gouda et al., 1992) provide circumstantial evidence that does not unambiguously demonstate a helical conformation for the third helix of the B domain in the B−Fc$_1$ complex. In addition, all published structural studies have been performed using isolated IgG-binding domains of SpA. Since there are two binding sites for SpA on each IgG molecule, a possible mechanism of binding of the five-domain SpA molecule to Fc would involve third-helix unwinding of one IgG-binding domain to allow for the polypeptide chain to extend and allow binding of the neighboring domain on the other side of the Fc molecule. By this mechanism, the helix unwinding would be cooperatively driven by IgG binding on both sides of the Fc molecule.

We have undertaken a mutagenesis, biophysical, and structural study of domain Z, an analogue of domain B that was constructed for protein engineering and gene fusion purposes (Nilsson et al., 1987). In this engineered SpA domain, the binding surface for IgG was maintained from domain B, but a glycine residue was replaced by an alanine residue in helix 1 and the gene encoding Z was constructed to allow for obligate head-to-tail polymerizations. Domain Z has been shown to possess full Fc$_1$ binding affinity (Ljungberg et al., 1993). In a recent mutagenesis study, it was demonstrated that substitutions of other residues in domain Z (e.g., Leu^{17}Asp, Asn^{28}Ala, Ile^{31}Ala, and Lys^{35}Ala),[2] all present in the suggested binding surface to Fc, results in decreased binding affinity (Cedergren et al., 1993). These findings are completely consistent with the binding surface indicated by the X-ray structure of the B−Fc$_1$ complex (Deisenhofer, 1981). Surprisingly, when the binding kinetics of these mutant domain Z proteins were analyzed, it was found that two of the substitutions in Z (Leu^{17}Asp and Ile^{31}-Ala), which have decreased affinity for Fc, are affected mainly in the on-rate of binding (k_{on}). In contrast, other substitutions (e.g., Asn^{28}Ala and Lys^{35}Ala) affect the binding constant by increasing the off-rate (k_{off}) (Jendeberg et al., 1995). From these results it was proposed that there are possible structural changes in the Z domain upon binding to Fc.

In the present study, we specifically address the proposed helical unwinding in domain Z upon binding to Fc using CD spectroscopy. First, solution NMR spectroscopy was used to determine the backbone chain fold of domain Z in solution. It was found that domain Z is an antiparallel three-helical bundle structure similar to that of domain B (Torigoe et al., 1990a; Gouda et al., 1992). Having characterized the overall structure of Z in its unbound state, we next used circular dichroism (CD) spectroscopy to identify changes in α-helical content of Z or ZZ, a two-domain Z tandem repeat, upon binding to Fc$_1$, respectively. On the basis of these results, we demonstrate that there is no disruption of the three-helical backbone structure of Z in the binding process.

MATERIALS AND METHODS

Materials. A monovalent form of a one-domain protein A analogue, consisting of 58 amino acids designated Z (Nilsson et al., 1987), was used in this study. The Z protein used in the NMR analysis has an N-terminal extension of 14 amino acid residues (Cedergren et al., 1993). This amino acid sequence extension has no detectable effect on Fc affinity or on the kinetics of Fc binding (L. Jendeberg and B. Nilsson, unpublished data). Isotope-enriched Z domain samples for NMR studies were produced in an *Escherichia coli* intracellular production system under the control of the *trp* promoter (Cedergren et al., 1993). Details of the

[2] In this paper, amino acid residues are numbered from the N-terminus corresponding to their positions in domain B of staphylococcal protein A according to Cedergren et al. (1993). Amino acid substitutions are designated by the amino acid residue in the parent protein, the amino acid number, and then the amino acid residue substitution, e.g., Leu^{17}Asp for leucine 17 substituted with an aspartic acid residue.

fermentation and purification procedures are presented elsewhere (Cedergren et al., 1993; Lyons et al., 1993; Jansson et al., 1995). The yields of purified [^{15}N]Z and [^{15}N,^{13}C]Z were approximately 40 mg/L of culture volume in shaker flasks using 4 g/L of glucose or [^{13}C]glucose, respectively, and 2 g/L ($^{15}NH_4)_2SO_4$. The Z, ZZ, and Fc proteins used in the CD analysis were recombinant proteins produced in *E. coli* by secretion to the periplasm directed by the SpA signal peptide. These Z proteins both have a C-terminal extension of 17 amino acids (VDANSRGSVDLQPSLSK). Also, this amino acid sequence extension has no detectable effect on Fc affinity or kinetics of Fc binding (L. Jendeberg and B. Nilsson, unpublished data). All Z and ZZ proteins were purified by IgG affinity chromatography using IgG−Sepharose FF (Pharmacia Biotechnology, Uppsala, Sweden) as described elsewhere (Nilsson & Abrahmsén, 1990). The proteins were then further purified by gel filtration using Sephadex G-50 SF (Pharmacia Biotechnology). The recombinant Fc_1 protein utilized in the CD study was a functional Fc_1 analogue in terms of SpA binding. It consists of the hinge region and framework amino acids from human Fc_3 and the SpA-binding region from Fc_1. The molecule has full binding to SpA and streptococcal protein G (details to be published elsewhere). The proteins were purified by protein G−Sepharose FF (Pharmacia Biotechnology) affinity chromatography according to the supplier's recommendations, with elution in 0.5 M acetic acid, pH 2.7. Buffer exchange was performed using a fast desalting column, G-25 (Pharmacia Biotechnology).

Analysis of Purified Proteins. Purified proteins were analyzed by SDS−PAGE using the Phast system (Pharmacia Biotechnology). Amino acid compositions were determined by hydrolyzing each protein in 6 M HCl at 155 °C for 45 min followed by separation on an ion-exchange column and detection of amino acids by ninhydrin. The analyses were performed on a Beckman 6300 amino acid analyzer, equipped with a System Gold data handling system (Beckman).

NMR Spectroscopy. Samples for NMR spectroscopy were prepared in buffered solutions of either 100% ^2H_2O or 90% H_2O containing 10% ^2H_2O. Protein concentrations were 2−3 mM, and the solutions were buffered with 10 mM KH_2PO_4 containing 0.2 mM NaN_3 at pH 6.5 ± 0.1. NMR spectra were obtained with a Varian Unity 500 spectrometer system at temperature of 30 ± 0.1 °C. Two-dimensional NOE spectroscopy (NOESY) (Macura & Ernst, 1980) and pulsed-field gradient ^{15}N heteronuclear single quantum coherence spectroscopy (PFG-HSQC) (Li & Montelione, 1993) were carried out using previously described pulse sequences. NOESY data were recorded using 512 time-proportional phase increments over a 6150 Hz spectral width in the ω_1 dimension and 2048 complex data points over a 6000 Hz spectral width in the ω_2 dimension. Hydrogen/deuterium exchange measurements were recorded from freshly dissolved samples of the ^{15}N-enriched Z domain in ^2H_2O by obtaining a series of PFG-HSQC spectra over a 36 h period. Backbone vicinal coupling constants were estimated from HSQC-J spectra (Neri et al., 1990; Billeter et al., 1992) recorded with an array of mixing times, τ = 50, 56, 63, 71, 83, 100, 125, and 167 ms, corresponding to sign inversions for $^3J(H^N-H^\alpha)$ coupling constants of 10, 9, 8, 7, 6, 5, 4, and 3 Hz, respectively, as described elsewhere (Moy et al., 1993).

Structure Generation Calculations. Structure generation calculations were carried out by a hybrid approach in which structures were first generated using the DIANA program (Güntert et al., 1991) and then energy-refined by restrained simulated annealing with molecular dyanmics using the CONGEN computer program (Bruccoleri & Karplus, 1987, 1990; Bassolino-Klimas et al., 1995; Tejero et al., 1995) and the CHARMM (Brooks et al., 1983) potential function. Calculations were done using protocols similar to those described elsewhere (Bassolino-Klimas et al., 1995; Tejero et al., 1995). Briefly, 40 structures were first generated from random starting conformations using the DIANA package (Güntert et al., 1991) provided with Triad (Tripos, Inc.) molecular modeling software. These structures were then used as starting points for simulated annealing calculations with a restrained energy function. Initial atomic velocities were chosen randomly from a Maxwellian distribution at 1000 K. Molecular dynamics trajectories were then calculated for 24 ps at high temperature (1000 K) with high weights on covalent parameters (e.g., bond lengths and bond angles) while slowly increasing the weights on the distance and dihedral angle constraint terms of the target function (weight annealing). Next, a series of 12 1.0 ps molecular dynamics simulations were carried out at decreasing temperatures between 1000 and 300 K (temperature annealing). The normal CHARMM (Brooks et al., 1983) values for covalent geometries and final weights of 100 kcal mol^{-1} Å^{-2} and 100 kcal mol^{-1} rad^{-2} on the distance and dihedral angle terms of the target function were then used to calculate a 15 ps restrained MD trajectory at 300 K. Finally, the average coordinates during the last 3 ps of this final trajectory were computed and energy minimized with experimental constraints. The time step of the integrator was 1 fs in all molecular dynamics calculations. In all of the energy calculations, nonbonded interactions were included up to a cutoff of 10 Å, and electrostatic interactions were evaluated using a distance-dependent dielectric constant equal to the interatomic distance. The ten structures with lowest values of residual constraint violations were then selected to represent the solution stucture of the Z domain.

All computations were carried out on a Silicon Graphics Indigo 2$^+$ computer workstation. NMR spectra were processed and analyzed using VNMR (Varian Associates), NMRCompass (Molecular Simulations), and Triad (Tripos, Inc.) computer software. Superpositions of atomic coordinates by the method of Kabsch (1978) and statistical analyses of NMR structures were carried out using the ORIENT molecular graphics (G. Elkins and G. T. Montelione, unpublished) and PDBSTAT (R. Tejero and G. T. Montelione, unpublished) computer programs. These C programs are available upon request from the authors.

Preparation of Samples for CD Analysis. Samples for CD analysis were prepared in a 20 mM phosphate buffer at pH 6.5, supplemented with 0.05% Tween 80 (Kebo AB, Sweden). The protein concentrations used were for Fc 7.5 μM (0.40 mg/mL), for Z 7.5 and 15 μM (0.068 and 0.14 mg/mL), and for ZZ 7.5 and 3.8 μM (0.12 and 0.059 mg/mL). Mixtures of these proteins were prepared with molar ratios of 1:1 and 2:1 for Z to the Fc homodimers, respectively, and for ZZ together with the two Fc's in molar ratios of 1:1 and 0.5:1, respectively. Complex formation in these samples was monitored by native PAGE (pH 8.8) using the Phast system (Pharmacia Biotechnology). All protein concentrations were determined by quantitative amino acid composition analysis.

Circular Dichroism Spectroscopy. Far-UV CD spectra were collected in a J-720 spectropolarimeter (JASCO, Japan)

using wavelengths of 250−200 nm at room temperature. The scanning speed was 10 nm/min, and each spectrum was averaged from five scans. The optical path length was 1 mm. Differential CD spectra were calculated by subtracting relevant molar normalized primary CD spectra and thereafter conversion to mean residue ellipticitiy (deg × cm^2 × $dmol^{-1}$) for the remaining polypeptide (Z or ZZ, respectively).

RESULTS

SpA is a five-domain molecule, and a binding mechanism involving third-helix unwinding would allow neighboring domains of SpA to bind on *both* sides of Fc simultaneously. This hypothesis could explain the fact that a molecule composed of two fused domains of Z, designated ZZ, binds 20 times tighter than Z to Fc (Eliasson, 1990), although the affinity constant does not increase significantly further for larger constructs including up to five domains of Z (Eliasson, 1990). Recently, it was demonstrated that the previously defined tighter binding of ZZ is a result of a slower off-rate of binding (Jendeberg et al., 1995), which is consistent with the proposed mechanism. There are two symmetric binding sites on the homodimeric Fc molecule for domain B (or Z), and model building demonstrates that a partially unwound third helix of the ZZ molecule could conceivably span these two sites (data not shown). Similar, though weaker, interactions between the unwound third helices of domain B (or Z) and Fc_1 are also possible. In such a mechanism, the protected amide protons of the polypeptide segment Ser^{41}−Ala^{54} of the complexed domain B (Gouda et al., 1992) could be rationalized by an interaction of the unwound third helix with the Fc molecule itself. In order to evaluate this hypothesis, we determined the three-dimensional structure of the Z domain in solution and compared the backbone CD spectra of Z, ZZ, and complexes of these domains with recombinant Fc fragments of IgG antibodies.

Determination of the Overall Polypeptide Chain Fold of Domain Z by NMR. Sequence-specific assignments for most proton and nitrogen resonances of domain Z have been reported elsewhere (Lyons et al., 1993). Internuclear distance measurements were made from NOESY spectra of samples dissolved in H_2O and ^2H_2O recorded with mixing times τ_m of 50 ms. Locations of helical backbone conformation along three segments of the polypeptide sequence were first identified using characteristic patterns of strong H^N_i−H^N_{i+1}, weak to medium intensity H^α_i−H^N_{i+3}, and weak to medium intensity H^α_i−H^β_{i+3} NOEs, together with stretches of $^3J(H^N$−$H^\alpha)$ coupling constants less than 5 Hz (Wüthrich, 1986). Seventeen H^α_i−H^β_{i+3} NOEs were identified in these three helices, allowing their identification as α-helices rather than 3_{10} helices (Wüthrich et al., 1984; Wüthrich, 1986). This distinction was supported by structure generation calculations (described below), which demonstrate that all of the 66 interhelical NOEs are consistent with packing between α-helices rather than 3_{10} helices. The three α-helices of domain Z were corroborated by identifying slowly exchanging amide protons associated with their intrahelical hydrogen bonds. On the basis of these data, regular α-helical backbone conformations were assigned to three polypeptide segments: Lys^7 to His^{18} (helix 1), Glu^{25} to Asp^{36} (helix 2), and Ser^{41} to Ala^{54} (helix 3).

NOESY cross-peak intensities were calibrated using known distances within these helices. In the 50 ms H_2O NOESY spectrum, the average intensities for each class of NOEs, H^N_i−H^N_{i+1}, H^N_i−H^α_i, and H^α_i−H^N_{i+1}, within the α-helical polypeptide segments were assigned to the corresponding distances in an ideal α-helix (Wüthrich et al., 1984) and then used to calibrate a cross-peak intensity (I) vs distance (r) relationship, $I \propto 1/r^6$. These interproton distances span a range of both short and long distances and are highly consistent within regular α-helical structure. The corresponding NOEs are determined also by the overall tumbling of the polypeptide backbone and are minimally affected by side-chain dynamics. For proteins containing relatively long, regular α-helices like those of Z domain, these calibration distances are preferable to use compared with fixed aliphatic methylene or aromatic proton−proton distances of side chains. This calibration was then transferred to the 50 ms ^2H_2O spectrum using the intensities of NOESY cross-peaks between aromatic and aliphatic resonances which are common to both the H_2O and ^2H_2O data sets. All of the NOESY cross-peaks which could be assigned unambiguously in these two spectra were then converted into internuclear distances and used as upper-bound distance constraints for structure calculations. Finally, the resulting distance constraint list was filtered to remove entries which did not restrict the conformational space available to the computed protein structure.

A family of three-dimensional solution structures of domain Z was calculated using DIANA target function minimization (Güntert et al., 1991), followed by simulated annealing with CONGEN (Bassolino-Klimas et al., 1995; Tejero et al., 1995). As few NOE constraints were obtained for the 14 amino acid leader sequence of Z [i.e., polypeptide segment Met^{-14}−Ala^{-1}], the structural analysis was done only for the 58 amino acid segment Val^1−Lys^{58}. A total of 599 NMR-derived conformational constraints were used as input in these structure calculations, including (i) 468 upper-bound proton−proton distance constraints derived from 2D NOESY spectra, (ii) 100 upper- and lower-bound constraints indicated by 25 interstrand hydrogen bonds identified by amide $^1H/^2H$ exchange measurements, and (iii) 31 constraints on backbone dihedral angles ϕ which were restricted to the range $-160° < \phi < -80°$ and $-90° < \phi < -60°$ for vicinal $^3J(H^N$−$H^\alpha)$ coupling constants greater than 8 Hz and less than 5 Hz, respectively. Of these, there were 66 long-range constraints [i.e., $|i - j| > 5$ residues] which define the relative orientations of helices in these structures.

The resulting CONGEN structures satisfy the complete set of experimental constraints, with no distance constraint violations >0.3 Å or dihedral angle violations >5° (Table 1). These structures also exhibit good values of van der Waals (VDW E −2.3 to −3.4 kcal mol^{-1} $residue^{-1}$) and total conformational energies (conf E −12.2 to −16.3 kcal mol^{-1} $residue^{-1}$), as summarized in Table 1, and exhibit reasonably good covalent geometry (Table 2), with all peptide dihedral angles ω at 180 ± 5°.

The Z domain adopts a highly ordered three-helical bundle chain fold. A stereo diagram showing superpositions of backbone coordinates for the ten CONGEN structures is shown in Figure 2.[3] For the well-defined portions of the polypeptide chain (i.e., residues Phe^5−Ala^{56}), the rms deviations (relative to the mathematical average structure) for backbone and all heavy atoms are 0.83 and 1.50 Å,

[3] Throughout the text, "backbone atoms" refer to the N, C^α, and C′ atoms of the polypeptide chain.

Table 1: Summary of Residual Constraint Violations and Final Energies for Ten CONGEN NMR Structures of SpA Domain Z Determined at pH 6.5 and a Temperature of 30 °C

	structure									
	1	2	3	4	5	6	7	8	9	10
distance constraint violations										
>0.3 Å	0	0	0	0	0	0	0	0	0	0
0.2−0.3 Å	3	4	4	4	3	4	5	6	4	3
0.1−0.2 Å	16	14	15	15	13	14	15	10	11	13
<0.1 Å	19	22	20	24	23	21	22	24	19	30
total	38	40	39	43	39	39	42	40	34	46
dihedral angle constraint violations										
>5°	0	0	0	0	0	0	0	0	0	0
0−5°	2	2	2	2	3	3	0	5	1	2
energies[a]										
VDW E (kcal/mol)	−182	−188	−164	−169	−196	−181	−152	−134	−185	−190
conf E (kcal/mol)	−882	−913	−921	−775	−948	−854	−923	−707	−944	−898

[a] Energies were calculated using the CHARMM potential energy function (Brooks et al., 1983) with a cutoff of 10 Å. Both the total conformational energy (conf E), including electrostatic interactions, and van der Waals energy (VDW E), computed from the Lennard-Jones portion of the potential function, are reported for each structure.

Table 2: Summary of Structural Statistics for Ten CONGEN NMR Structures of Domain Z at pH 6.5 and a Temperature of 30 °C

rms deviations from ideal polypeptide geometry	
bond lengths	0.014 Å
bond angles	3.52°
peptide bond (improper constraints)	1.03°
peptide bond (ω dihedral)	2.66°
rms distance constraint violation	0.0382 Å
rms dihedral constraint violation	0.57°

respectively. The identification of α-helices in polypeptide segments Lys[7] to His[18], Glu[25] to Asp[36], and Ser[41] to Ala[54] was confirmed in these CONGEN structures by analysis of the corresponding ϕ and ψ backbone dihedral angles. For the α-helical core (i.e., residues 7−18, 25−36, and 41−54) the rms deviations for backbone and all heavy atoms are 0.55 and 1.27 Å, respectively. This structural analysis by NMR provides a reliable determination of the overall polypeptide chain fold of domain Z and clearly demonstrates the presence of a helical conformation for polypeptide segment Ser[41] to Ala[54].

Preparation of Mixtures of Z or ZZ with Fc_1 and Fc_3, Respectively. Recombinant Z, ZZ, Fc_1, and Fc_3 were produced in *E. coli* and purified to homogeneity. These proteins were mixed in order to monitor structural changes in Z or ZZ upon binding to Fc_1 using CD spectroscopy. Both Z and ZZ were studied since a two-domain molecule could be necessary to induce unwinding of the third helix by binding on both sides of Fc. Fc_3 was used as a control in all analyses since it is known not to bind SpA (Langone, 1982). In the CD analysis, different molar ratios of Z or ZZ to Fc proteins were used. For Z, ratios of 1:1 and 2:1 were used to verify the two potential binding sites on each Fc_1 molecule. Note that the Fc molecule is a homodimer where each monomer has two immunoglobulin domains (CH2 and CH3). For ZZ, molar ratios with Fc_1 and Fc_3 of 0.5:1 and 1:1 were used to address if a single ZZ molecule can occupy both binding sites on Fc_1. Prior to the CD analyses, complex formations between Z and ZZ with Fc_1 and Fc_3, respectively, were confirmed using a native 8−25% gradient polyacrylamide gel. The analysis with Z is shown in Figure 3; a complex between Fc_1 and Z was quantitatively formed as demonstrated by the disappearance of the Z band and a slight mobility shift of the Fc_1 band. As expected, by the same criteria there is no complex formation with Fc_3 (Figure 3). Complex formations were also obtained for the 2:1 ratio of Z:Fc_1 and for the two ratios of ZZ:Fc_1 (data not shown). From this gel analysis we conclude that both Z and ZZ bind to Fc_1 at both molar ratios and under the conditions used, respectively, but, as expected, no binding was detected to Fc_3 under these conditions.

Analysis of CD Spectra. CD spectra for domains Z or ZZ were collected together with spectra for Fc_1 and Fc_3 alone, as well as the mixtures with Z or ZZ at the molar ratios described above. The strategy used in collecting and analyzing these CD data is presented in Figure 4. The spectra for these mixtures were collected over the wavelength range from 250 to 200 nm. Data collection at lower wavelengths was hindered by the high concentration of proteins (0.5 mg/mL) used to obtain sufficient CD signal.

The CD spectra for Z, ZZ, Fc_1, and Fc_3, together with their respective mixtures, are shown in Figure 5. In order to compare the relative α-helical content of Z and ZZ in the free and bound state, the respective Fc spectrum was subtracted from the spectra of the mixtures, as outlined in Figure 4 and described in Materials and Methods.

The difference CD spectra as well as spectra of Z and ZZ alone are shown in Figure 6. The α-helical content was analyzed by the CD amplitude at 222 nm. These are similar in both the free and bound states. Therefore, we conclude that none of the three helices of Z or six helices of ZZ unwind upon binding to Fc_1. The control experiments exhibit no significant differences in the CD spectra of Z and ZZ with and without Fc_3 (Figure 6).

DISCUSSION

Polypeptide Chain Fold of Domain Z in Solution. In this paper we have studied the binding mechanism of an analogue based on staphylococcal protein A, designated Z, to Fc_1, in order to determine if an α-helix of Z is unfolded in the binding mechanism. The first goal was to determine that domain Z has a three-helical bundle chain fold similar to that of domain B. The overall chain fold of Z was determined from NMR data using DIANA followed by constrained simulated annealing. All of the structures calculated from the NMR constraints converge to a set of similar three-dimensional structures (Figure 2). The same results were obtained using extended starting conformations with random initial velocities as starting points for simulated annealing (data not shown). The structure of domain Z contains three well-defined α-helices: polypeptide segments

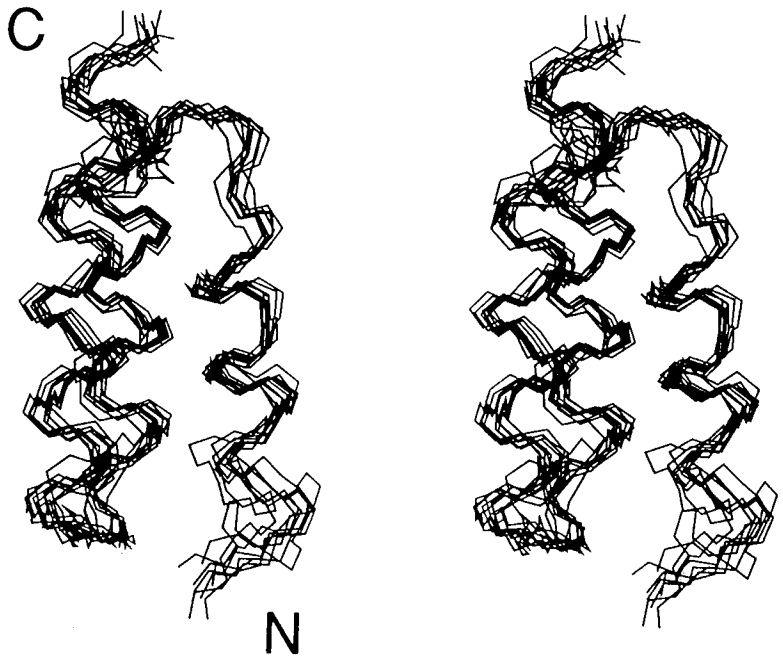

FIGURE 2: Stereo pairs showing optimized superpositions of backbone atoms (N, C^{α}, C′) for ten CONGEN structures of residues 5−56 of domain Z, showing the three-helical bundle chain fold.

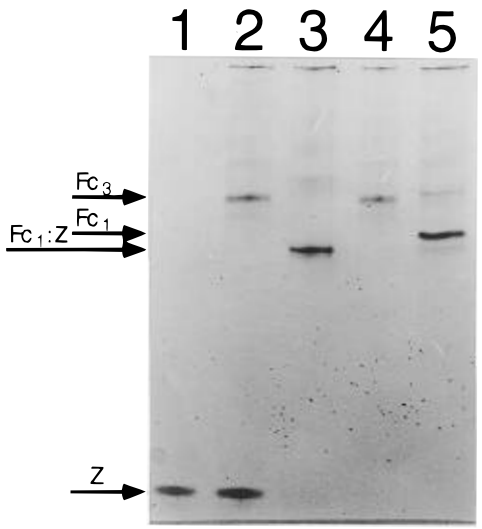

FIGURE 3: An 8−25% PAGE under native conditions of samples analyzed by CD spectroscopy (Figure 5A). Lanes: 1, Z; 2, mixture of Z and Fc_3 at a molar ratio of 1:1; 3, mixture of Z and Fc_1 at a molar ratio of 1:1; 4, Fc_3; 5, Fc_1.

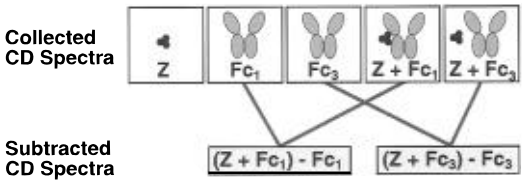

FIGURE 4: Strategy for collection and analysis of CD spectra used to characterize conformational changes in domain Z which accompany binding to Fc. The CD spectra of the individual components, as well as mixtures of these, are collected. Thereafter, the molar normalized spectrum of Fc (Fc_1 or Fc_3, respectively) is subtracted from the corresponding spectrum of each mixture. The resulting spectra are compared with the spectrum of Z or ZZ, respectively, alone.

Lys^{7} to His^{18} (helix 1), Glu^{25} to Asp^{36} (helix 2), and Ser^{41} to Ala^{54} (helix 3). The relative orientations of these helices are determined by 66 tertiary NOE constraints. Helices 2 and 3 are oriented almost perfectly antiparallel ($\Omega \approx 180°$), while helix 1 is approximately antiparallel to helix 2 but tilted by about 10°. The overall chain fold of domain Z determined by NMR is shown in Figure 7A. It can be compared with the 2.8 Å crystal structure of domain B bound to Fc_1 (Deisenhofer et al., 1981) shown in Figure 7B, which contains only two α-helices (i.e., helices 1 and 2) that are oriented nearly perfectly antiparallel ($\Omega \approx 180°$).

The NMR structure of Z at pH 6.5 described in this paper is also similar to the NMR solution structure recently described for domain B (Gouda et al., 1992) at pH 5.0 and a temperature of 30 °C. The NMR structure of domain B is based on 692 conformational constraints. Since atomic coordinates for domain B are not available, we cannot make a reliable comparison of these independently determined solution structures of two related SpA-derived domains. However, one significant difference involves the relative orientations of helix 1 with respect to helices 2 and 3. In the solution NMR structure of domain Z, helix 1 is tilted slightly ($\Omega \approx -170°$) with respect to the parallel axes of helices 2 and 3, while in the solution NMR structure of domain B (Gouda et al., 1992) the tilt of helix 1 with respect to helices 2 and 3 is much more pronounced ($\Omega \approx -150°$). The significance of this difference is not yet certain and awaits a detailed comparison of refined structures of the Z and B domains. The NMR structure refinement of domain Z is still in progress, and a more detailed description of its tertiary structure will be presented at a later date.

CD Studies of the Interactions between Z, ZZ, Fc_1, and Fc_3. Having established a three-helical bundle chain fold for domain Z in solution by NMR spectroscopy, we next used CD spectroscopy to evaluate structural changes associated with binding to the Fc_1 immunoglobulin domain. By comparison of the CD spectra of individual components (Z, ZZ, Fc_1, and Fc_3) as well as mixtures of Z or ZZ and Fc_1 or Fc_3, the average secondary structure contents could be monitored in the binding process. Secondary structure prediction algorithms are not recommended if CD data are not available below 200 nm (Johnsson, 1990). However, the α-helical content of a protein, with limited amounts of other secondary structural elements, can rather accurately

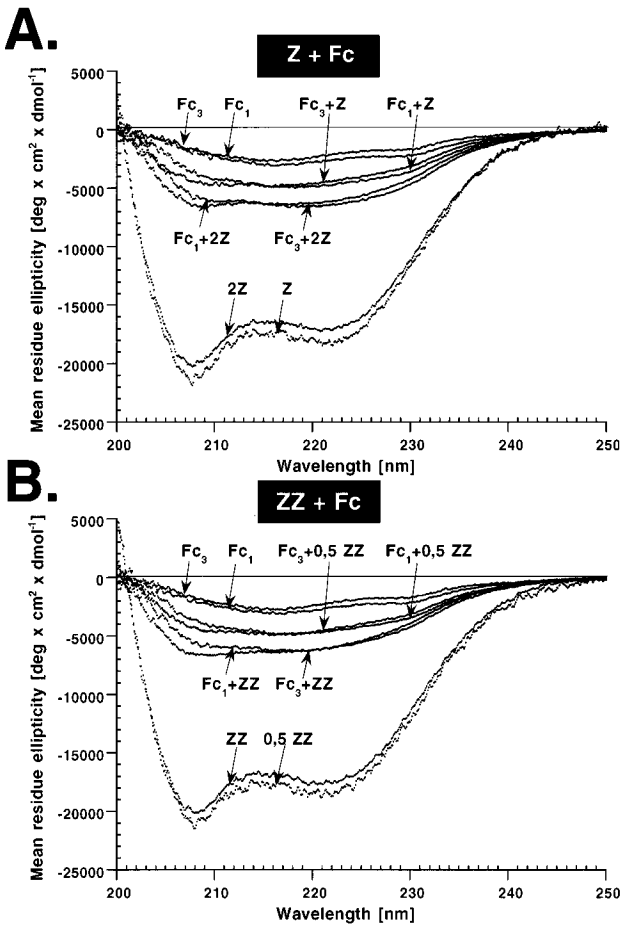

FIGURE 5: Superposition of CD spectra of proteins and protein mixtures. (A) Z, Fc_1, and Fc_3 and mixtures thereoff. Fc_n + Z, Z and Fc_n were mixed at an equimolar ratio; Fc_n + 2Z, Z and Fc_n were mixed at a molar ratio of 2:1; *n* is 1 or 3. (B) ZZ, Fc_1, and Fc_3 and mixtures thereoff. Fc_n + ZZ, ZZ and Fc_n were mixed at an equimolar ratio; Fc_n + 0.5ZZ, ZZ and Fc_n were mixed at a molar ratio of 0.5:1; *n* is 1 or 3. Note that Z or ZZ do not interact with Fc_3 (Figure 3).

be estimated by the molar ellipticity amplitude at 222 nm (Lifson & Roig, 1961; Johnson, 1990). This is a characteristic wavelength for α-helices, whereas other secondary structure elements, such as β-sheet, turn, or random coil, display only small CD signals at this wavelength [for a review, see Johnson (1990)]. Therefore, the application of CD spectroscopy to follow possible changes in α-helicity is particularly suitable in these mixtures since Fc is a β-sheet protein (Deisenhofer et al., 1978) with a small molar ellipticity CD signal at 222 nm (Figure 5). Thus, any disruption of helix 3 of Z into either random coil or extended conformations would change the CD amplitude at 222 nm significantly even for a complex with Fc. CD spectra were recorded on Fc_1 and Fc_3, respectively, and mixed separately with either Z or ZZ (Figure 5). The Fc_3 experiment was performed to address possible artifacts in terms of changes in CD upon mixing the two types of molecules, since SpA is known not to bind human Fc of subclass 3 (Langone, 1982). Indeed, gel electrophoresis analysis of the mixtures used in the CD analysis of Z with either Fc_1 or Fc_3 showed that a quantitative complex is formed between Z and Fc_1 and that Z and Fc_3 do not interact (Figure 3). Subsequently, the CD spectrum of the Fc molecule used in each analysis respectively was subtracted from the CD spectra of the mixtures (as outlined in Figure 4). The resulting difference spectra should display an unaltered Z (or ZZ) spectrum if no structural changes occur in Z (or ZZ) and Fc. In fact, this is exactly what is observed for the experiment with Fc_3, showing that the noncomplexed mixtures of Z (and ZZ) with Fc_3 are unaffected in their CD spectra and, thus, not affected in their secondary structures (Figure 6). On the other hand, the complexes of Fc_1 with either Z or ZZ show no significant change at 222 nm but similar minor spectral changes below 215 nm. If the third helix was unfolded in any of these complexes, CD amplitude at 222 nm in the difference spectra of Figure 6 would have decreased by roughly 30%. The amplitudes of the bands at 208 and 222 nm of a CD spectrum have been shown to possess a similar dependence upon changes in α-helical contents (Kem et al., 1990). Further, there are no detectable differences between the residual molar ellipticity spectra of Z and ZZ for the different molar ratios used. Therefore, the change in amplitude only below 215 nm is not likely due to a decrease in α-helicity of the Z domain. This corroborates the hypothesis (Gouda et al., 1992) that the polypetide segment Ser^{41}−Ala^{54} remains helical in the Z−Fc and ZZ−Fc complexes. However, the slight perturbation of the difference CD spectra at higher energy wavelengths is concluded to be significant since it occurs for both complexed Z and ZZ but not in the controls with Fc_3.

The high-energy region of the peptide CD spectrum of α-helical proteins has been proposed to be affected by relative interhelical orientations (Cooper & Woody, 1990). This suggests that the observed changes in CD spectra associated with Z (and ZZ) binding to Fc_1 may arise from changes in helical packing of Z (and ZZ). Alternatively, these spectral differences may arise from interactions of side-chain chromophores of Z and Fc_1. A third explanation for changes in the high-energy region of these CD spectra is that there are changes to the secondary structures of the Fc_1 portion of the complex. However, this is unlikely since these CD amplitude changes correspond to almost the *whole* mean residue ellipticity for Fc in this portion of the spectra (see Figure 5). Thus, we conclude from analysis of these difference CD spectra that Z and ZZ may undergo minor structural changes upon binding to Fc_1 but that most of the third helix observed in solution remains intact in the complex.

Mechanism of Binding of Fc by SpA Domain Z. From our results we propose a mechanism of binding involving a small tilt of helix 1 and 2 in relation to each other, while maintaining a helical structure in polypeptide segment Ser^{41}−Ala^{54} (i.e., helix 3). In both the NMR solution structures of the Z and B (Gouda et al., 1992) domains, helix 1 is tilted with respect to the parallel axes of helices 2 and 3 by 10−30°. While the precise value of this tilt in domain Z is not yet certain, a parallel orientation of helix 1 ($\Omega \approx -180°$) is inconsistent with many of the interhelical NOE distance constraints obtained for the Z domain, including several NOEs from aromatic ring protons of residue Phe^5 (near the N-terminus of helix 1) to side-chain atoms of residues Leu^{34}, Lys^{35} (in helix 2), and Pro^{38} (between helix 2 and helix 3), and from the backbone amide group of Glu^{15} (in helix 1) to the methyl resonances of residue Leu^{45} (in helix 3). On the other hand, while the conformation of helix 3 is not defined in the crystal structure of the B−Fc_1 complex (Deisenhofer et al., 1981), the relative orientations of helices 1 and 2 are clearly antiparallel ($\Omega \approx -180°$) and significantly different from the relative orientations in the NMR solution structures, as can be seen by comparing the stereo diagrams shown in Figure 7.

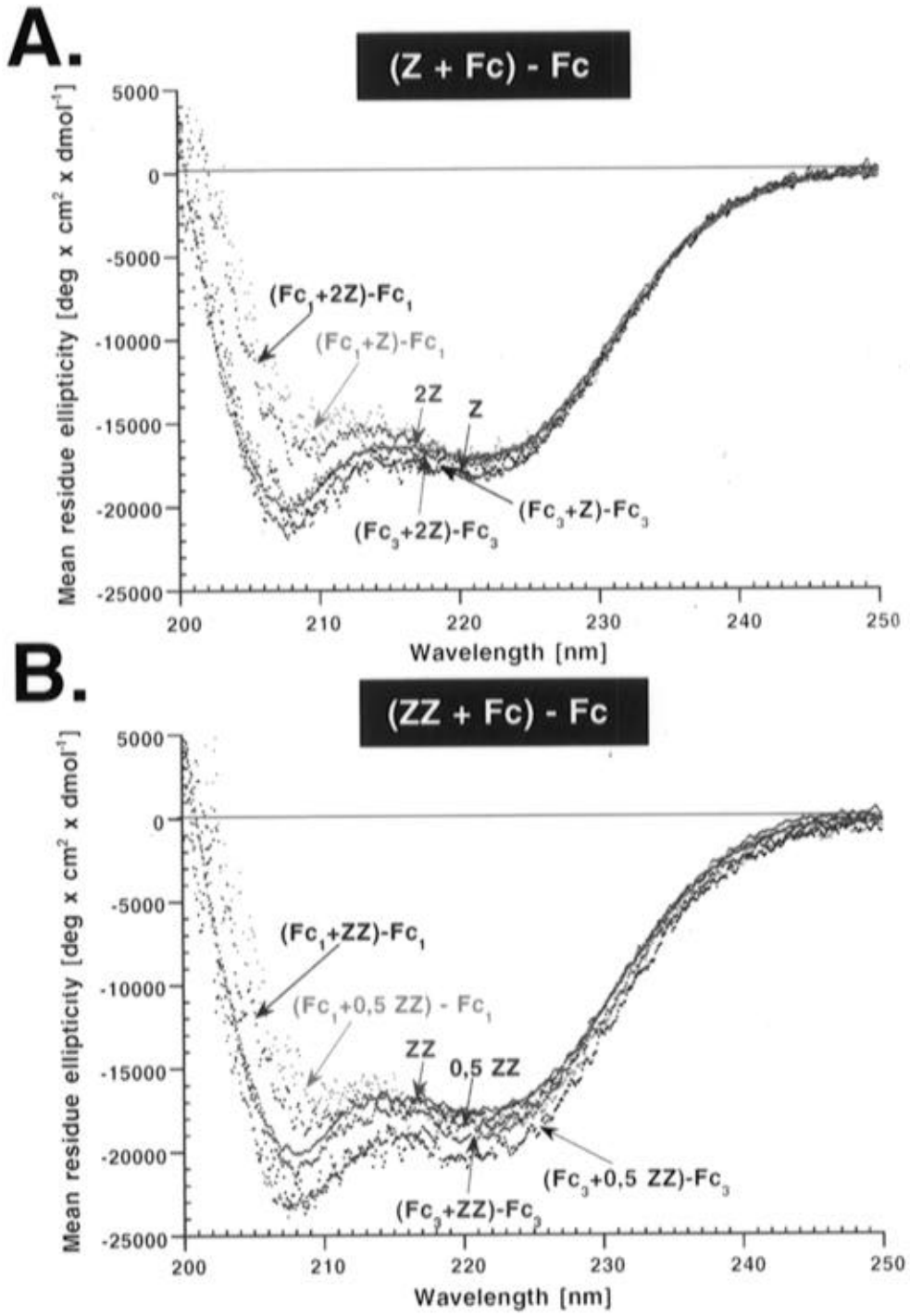

FIGURE 6: Superposition of CD spectra and subtracted CD spectra derived from the data shown in Figure 5. (A) Spectra of Z alone and Z in a mixture with Fc_n, where the Fc_n spectrum has been subtracted. (Fc_n + Z) − Fc_n, subtraction of the Fc_n spectrum from the spectrum collected for the equimolar mixture of Z and Fc_n; (Fc_n + 2Z) − Fc_n, subtraction of the Fc_n spectrum from the spectrum obtained for Z and Fc_n at a molar ratio of 2:1; *n* is 1 or 3. (B) Spectra of ZZ alone and ZZ in a mixture with Fc_n, where the Fc_n spectrum has been subtracted. (Fc_n + ZZ) − Fc_n, subtraction of the Fc_n spectrum from the spectrum collected for the equimolar mixture of ZZ and Fc_n; (Fc_n + 0.5ZZ) − Fc_n, subtraction of the Fc_n spectrum from the spectrum obtained for ZZ and Fc_n at a molar ratio of 0.5:1; *n* is 1 or 3. Note that Z or ZZ do not interact with Fc_3 (Figure 3).

This proposed binding mechanism involving minor reorientation of helices 1 and 2 is compatible with all published data. It would explain the rather slow on-rate of binding (10^5 M^{-1} s^{-1}), which is about 3 orders of magnitude slower than what is expected for a strict diffusion-controlled interaction (Jendeberg et al., 1995). A mechanism involving reorientation of helices 1 and 2 in the binding process could also account for the fact that mutations in the helix 1 and 2 interface ($Ile^{31}Ala$, $Leu^{17}Asp$) create even slower binders, while the destabilizing mutation $Phe^{30}Ala$ in the helix 2 and 3 interface does not affect binding energetics or kinetics (Cedergren et al., 1993; Jendeberg et al., 1995).

Why Is the Third Helix of the Complexed B Domain Not Observed in the X-ray Structure? The CD data presented in this paper indicate that the third helix of domain Z is in fact present in the Z−Fc_1 complex. These results support the view that retarded amide hydrogen/deuterium exchange rates for this polypeptide segment in the B−Fc_1 complex (Gouda et al., 1992) are in fact due to an intact third α-helix, rather than to interactions between B and Fc_1. Similar

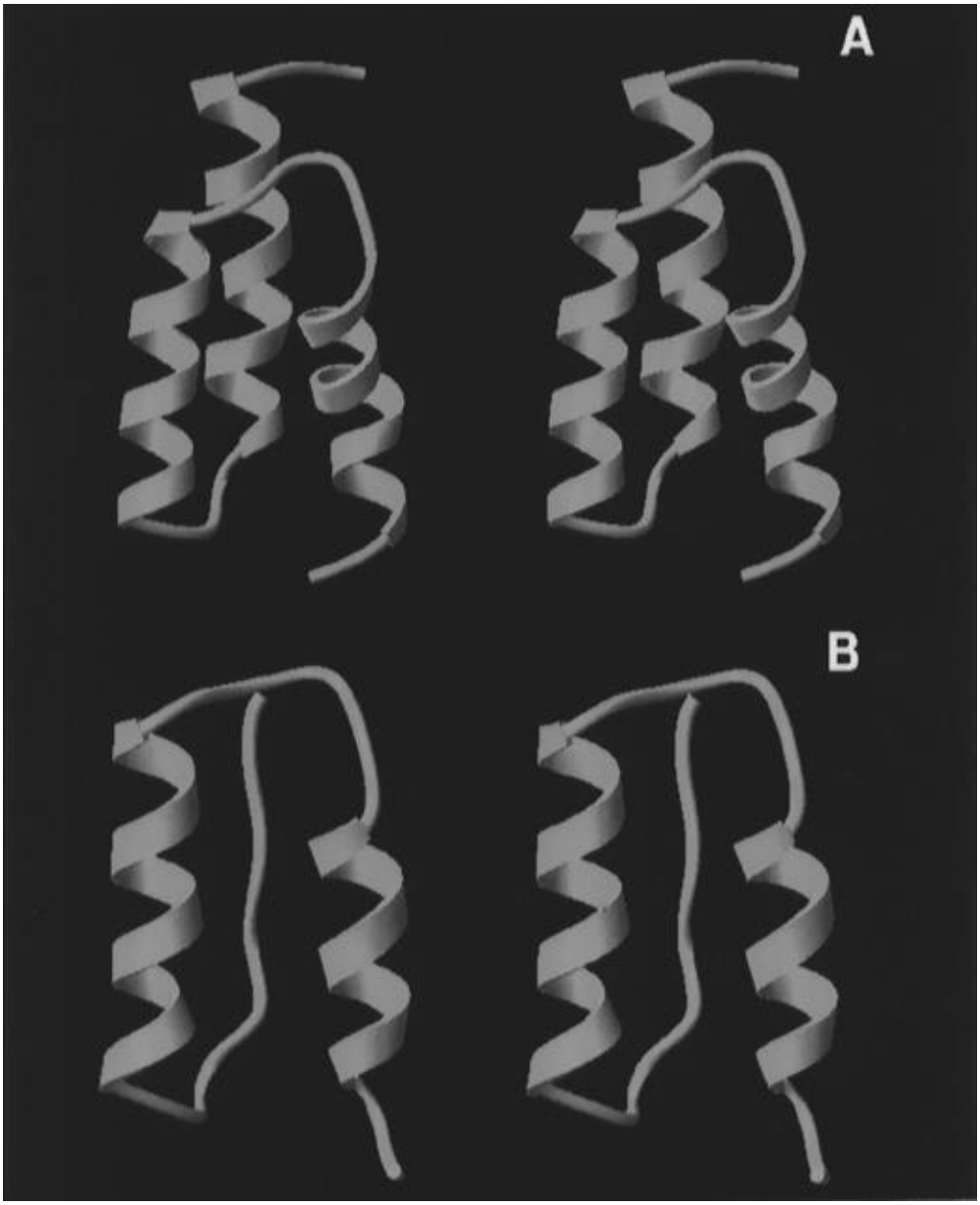

FIGURE 7: Ribbons (Carson et al., 1991) representations of SpA domain structures. (A) NMR solution structure of domain Z at pH 6.5. (B) Bound state conformation of domain B of SpA from the 1fc1 coordinates derived from the cocrystal structure of domain B and Fc_1 (Deisenhofer, 1981).

hydrogen/deuterium exchange studies on Z−IgG complexes also demonstrate that amide protons of helices 1, 2, and 3 are protected from rapid exchange (data not shown). However, these NMR and CD studies leave open the question of why helix 3 of the B domain is not observed in the crystal structure of the B−Fc_1 complex.

The absence of helix 3 in this crystal structure may be explained by several possible crystallographic artifacts. First, the crystal structure of the B−Fc_1 complex was refined only to 2.8 Å resolution (Deisenhofer, 1981) and exhibits relatively poor electron density. While the initial description of the complex at 3.5 Å resolution suggested that there might be a third helix (Deisenhofer et al., 1978), this feature was not described for the more refined 2.8 Å structure (Deisenhofer et al., 1981). A second possible explanation for the missing electron density is crystal packing interactions which may destabilize and partially unfold domain B in the crystalline environment (Gouda et al., 1992). Crystal packing interactions were described (Deisenhofer et al., 1981) between polypeptide segments Asp^{36}−Gln^{40} (near the N-terminus of helix 3 in the solution NMR structures of B and Z) of domain B and the CH3 portion of Fc_1 in the 2.8 Å structure of the complex. This crystal contact also includes a large peak of electron density which has been interpreted as a sulfate ion from the ammonium sulfate present in the crystallization solution (Deisenhofer et al., 1981). Crystal packing interactions at this site may be especially important as residue Gln^{40} acts as a potential N-cap residue for helix 3 in the solution NMR structure of domain Z. A third possible explanation for the discrepancy is that crystals used for crystallographic studies were produced at pH 4.1, while NMR and CD studies were carried out at pH 6.5. However, amide hydrogen/deuterium exchange NMR studies of Z demonstrate that all three helices are intact in the free state at pH 4.5 (data not shown). In addition, CD spectra of domain Z at pH's ranging from 2 to 7 are very similar (data not shown), indicating similar overall structures.

In addition to these technical explanations for the absence of helix 3 in the crystal structure of the complex, another

possible explanation comes from considerations of intramolecular dynamics. While the NMR and CD studies demonstrate that the third helix is present, it may be loosely packed against the other two helices and therefore may exist in two or more different tertiary conformations in the crystal. Potentially, the reorientation of helices 1 and 2 in forming the Fc_1 binding epitope would change the docking site for helix 3, resulting in a less stable interhelical packing interaction. In such a long-lived dynamic interaction with helices 1 and 2, helix 3 could still exhibit CD spectra and slowly exchanging amides characteristic of an α-helix. Interestingly, in PDB coordinates of the crystal structure (entry 1fc2 in the Brookhaven Protein Database) the polypeptide sequence corresponding to helix 3 of the solution structure starts out with defined helical ϕ, ψ values, but the electron density gets increasingly weaker along the polypeptide chain toward the C-terminus (Deisenhofer et al., 1981). This observation is compatible with our proposal, since an ensemble of different interhelical packing angles would result in the largest atomic displacements between conformational states at the C-terminal end of helix 3.

Mechanism of the ZZ−Fc_1 Interaction. The ZZ molecule was found to bind tighter than Z (Eliasson, 1990), and we have previously demonstrated that this is an off-rate effect (Jendeberg et al., 1995). Thus, the k_{off} of ZZ is about 6 times lower than the k_{off} of Z. ZZ cannot bind on both sides of Fc_1 since it cannot span the two binding sites on Fc without disrupting its third helix (modeling data not shown). Instead, we propose here that the uncomplexed Z domain of the ZZ molecule may interact weakly with the bound Z domain or with Fc_1 itself at a second binding site. Either of these possibilities could provide increased binding free energy and could result in a lowered k_{off}. However, more experiments will be necessary to completely characterize this co-operative binding effect of going from one to two domains of Z.

At present, we are in the process of refining the solution NMR structure of Z by including more constraints from multidimensional NMR analysis in order to better define the details of interhelical packing in solution. These structural data will be used to generate mutant Z molecules designed to favor the bound state conformation of Z in solution. Such molecules are expected to bind faster than the parent Z molecule to Fc_1 and would further corroborate our proposed mechanism of binding.

ACKNOWLEDGMENT

Drs. Tomas Lundqvist, Per-Åke Nygren, and Alexander Arseniev are acknowledged for fruitful discussions throughout the course of this project. Antonella Larsson and Per Denker are thanked for sharing their Fc production vectors.

REFERENCES

Bassolino-Klimas, D., Tejero, R., Krystek, S. R., Metzler, W. J., Montelione, G. T., & Bruccoleri, R. E. (1995) *Protein Sci.* (submitted for publication).

Bazan, J. F. (1990) *Proc. Natl. Acad. Sci. U.S.A. 87*, 6934−6938.

Billeter, M., Neri, D., Otting, G., Qian, Y. Q., & Wüthrich, K. (1992) *J. Biomol. NMR 2*, 257−274.

Brooks, B. R., Bruccoleri, R. E., Olafson, B. D., States, D. J., Swaminathan, S., & Karplus, M. (1983) *J. Comput. Chem. 4*, 187−217.

Bruccoleri, R. E., & Karplus, M. (1987) *Biopolymers 26*, 137−168.

Bruccoleri, R. E., & Karplus, M. (1990) *Biopolymers 29*, 1847−1862.

Carson, M. (1991) *J. Appl. Crystallogr. 24*, 958−961.

Cedergren, L., Andersson, R., Jansson, B., Uhlén, M., & Nilsson, B. (1993) *Protein Eng. 6*, 441−448.

Cooper, T. M., & Woody, R. W. (1990) *Biopolymers 30*, 657−676.

Cunningham, B. C., & Wells, J. A. (1993) *J. Mol. Biol. 233*, 554−563.

Deisenhofer, J. (1981) *Biochemistry 20*, 2361−2370.

Deisenhofer, J., Colman, P. M., Epp, O., & Huber, R. (1976) *Hoppe-Seyler's Z. Physiol. Chem. 357*, 1421−1434.

Deisenhofer, J., Jones, T. A., Huber, R., Sjödahl, J., & Sjöquist, J. (1978) *Hoppe-Seyler's Z. Physiol. Chem. 359*, 975−985.

Eliasson, M. 1990 Streptococcal protein G—Structure and function, Ph.D. Thesis, Royal Institute of Technology, Stockholm, Sweden (ISBN 91-7170-012-9).

Gouda, H., Torigoe, H., Saito, A., Sato, M., Arata, Y., & Shimada, I. (1992) *Biochemistry 31*, 9665−9672.

Güntert, P., Braun, W., & Wüthrich, K. (1991) *J. Mol. Biol. 217*, 517−530.

Jansson, B., Palmcrantz, C., Uhlén, M., & Nilsson, B. (1989) *Protein Eng. 2*, 555−561.

Jansson, M., Li, Y.-C., Jendeberg, L., Anderson, S., Montelione, G. T., & Nilsson, B. (1995) *J. Biomol. NMR* (in press).

Jendeberg, L., Persson, B., Andersson, R., Karlsson, R., Uhlén, M., & Nilsson, B. (1995) *J. Mol. Recognit.* (in press).

Johnson, W. C., Jr. (1990) *Proteins 7*, 205−214.

Kabsch, W. (1978) *Acta Crystallogr., Sect. A 34*, 827−828.

Kem, W. R., Tu, C.-K., Williams, R. W., Toumadje, A., & Johnson, W. C. (1990) *J. Protein Chem. 9*, 433−443.

Langone, J. J. (1982) *Adv. Immunol. 32*, 157−252.

Li, Y.-C., & Montelione, G. T. (1993) *J. Magn. Reson. B101*, 315−319.

Lifson, S., & Roig, A. (1961) *J. Chem. Phys. 34*, 1963−1974.

Ljungberg, U. K., Jansson, B., Niss, U., Nilsson, R., & Nilsson, B. (1993) *Mol. Immunol. 30*, 1279−1285.

Lyons, B. A., Tashiro, M., Cedergren, L., Nilsson, B., & Montelione, G. T. (1993) *Biochemistry 32*, 7839−7845.

Macura, S., & Ernst, R. R. (1980) *Mol. Phys. 41*, 95−117.

Moy, F. J., Li, Y., Rauenbuehler, P., Winkler, M. E., Scheraga, H. A., & Montelione, G. T. (1993) *Biochemistry 32*, 7334−7353.

Neri, D., Otting, G., & Wüthrich, K. (1990) *J. Am. Chem. Soc. 112*, 3663−3665.

Nilsson, B., & Abrahmsén, L. (1990) *Methods Enzymol. 185*, 145−161.

Nilsson, B., Moks, T., Jansson, B., Abrahmsén, L., Elmblad, A., Holmgren, E., Henrichson, C., Jones, T. A., & Uhlén, M. (1987) *Protein Eng. 1*, 107−113.

Rozwarski, D. A., Gronenborn, A. M., Clore, G. M., Bazan, J. F., Bohm, A., Wlodawer, A., Hatada, M., & Karplus, P. A. (1994) *Structure 2*, 159−173.

Tejero, R., Bassolino-Klimas, D., Bruccoleri, R. E., & Montelione, G. T. (1995) *Protein Sci.* (submitted for publication).

Torigoe, H., Shimada, I., Saito, A., Sato, M., & Arata, Y. (1990a) *Biochemistry 29*, 8787−8793.

Torigoe, H., Shimada, I., Waelchli, M., Saito, A., Sato, M., & Arata, Y. (1990b) *FEBS Lett. 269*, 174−176.

Uhlén, M., Guss, B., Nilsson, B., Gatenbeck, S., Philipson, L., & Lindberg, M. (1984) *J. Biol. Chem. 259*, 1695−1702.

Wüthrich, K. (1986) *NMR of Proteins and Nucleic Acids*, Wiley, New York.

Wüthrich, K., Billeter, M., & Braun, W. (1984) *J. Mol. Biol. 180*, 715−740.

BI9512814